



HAL
open science

The effects of solid barriers and blocks on the propagation of smoke within longitudinally ventilated tunnels

Fateh Chaabat, Mathieu Creyssels, Antoine Mos, Joy Wingrave, Horacio Correia, Massimo Marro, Pietro Salizzoni

► **To cite this version:**

Fateh Chaabat, Mathieu Creyssels, Antoine Mos, Joy Wingrave, Horacio Correia, et al.. The effects of solid barriers and blocks on the propagation of smoke within longitudinally ventilated tunnels. *Building and Environment*, 2019, 160, pp.106207. 10.1016/j.buildenv.2019.106207 . hal-03158114

HAL Id: hal-03158114

<https://hal.science/hal-03158114>

Submitted on 25 Oct 2021

HAL is a multi-disciplinary open access archive for the deposit and dissemination of scientific research documents, whether they are published or not. The documents may come from teaching and research institutions in France or abroad, or from public or private research centers.

L'archive ouverte pluridisciplinaire **HAL**, est destinée au dépôt et à la diffusion de documents scientifiques de niveau recherche, publiés ou non, émanant des établissements d'enseignement et de recherche français ou étrangers, des laboratoires publics ou privés.



Distributed under a Creative Commons Attribution - NonCommercial 4.0 International License

1 *The Effects of Solid Barriers and Blocks on the Propagation of Smoke Within* 2 *Longitudinally Ventilated Tunnels*

3 **Chaabat¹, F., Creyssels¹, M., Mos², A., Wingrave¹, J., Correia¹, H., Marro¹, M., Salizzoni¹, P.,**

4 ¹*Laboratoire de Mécanique des Fluides et d'Acoustique, University of Lyon, CNRS UMR 5509 Ecole Centrale*
5 *de Lyon, INSA Lyon, Université Claude Bernard, 36, avenue Guy de Collongue, 69134 Ecully, France*

6 ²*Centre d'Etudes des Tunnels, avenue François Mitterrand, 69500 Bron, France*

7 **ABSTRACT**

8 A series of experiments were conducted to investigate the effect of solid barriers, placed at the tunnel ceiling, on the
9 behaviour of smoke in fire events within longitudinally ventilated tunnels, namely on the smoke back-layering lengths and on
10 the critical velocity. For this purpose, we considered two types of barrier: "small barriers" designed to be fixed in place and
11 "large barriers" designed to be mobile in real tunnels. The study was carried out in a small scale tunnel, by simulating fire
12 smokes with a light gas mixture of air and helium. Experiments were performed with and without blocks within the tunnel,
13 representing vehicles. Results show that the presence of barriers and/or blocks prevents the smoke back-layering flow,
14 therefore reducing the critical velocity. The reduction rate of the latter depends on the blocking rate created by the obstacles
15 (barriers, blocks or both) located just upstream of the source.

16 Further experiments were conducted to investigate the effects of blockages on pressure losses inside the tunnel. The results
17 reveal a proportionality between head losses and height of barriers, and between pressure drops and size of the blocks. When
18 both blocks and barriers are present, the pressure losses induced by the small barriers are very high compared to those
19 induced by the large barriers, especially in the tunnel with large blocks. These findings suggest that large barriers are more
20 effective than small ones because they prevent the smoke back-layering at very low critical velocities and they induce less
21 pressure losses in congested tunnels.

22 *Keywords:* Tunnel ventilation, Solid barriers, Blocks, Buoyant plume, Back-layering, Critical velocity, Pressure losses.

23 **NOMENCLATURE**

24 **Roman and Greek Symbols**

25	H	Height of the tunnel (m)
26	W	Width of the tunnel (m)
27	\bar{D}	Hydraulic diameter of the tunnel (m)
28	h	Barrier height (m)
29	D_i	Diameter of the source (m)
30	L	Smoke back-layering flow length (m)
31	L_{1-2}	Distance between the two pressure measurement points P1 and P2 (m)
32	d	Distance between a large barrier and the source (m)
33	S	Spacing between each two adjacent small barriers (m)
34	Δp	Pressure difference (Pascal)
35	g	Gravity acceleration (m/s^2)
36	ρ	Density (kg/m^3)
37	q	Volume flow (m^3/s)
38	B_i	Buoyancy flux (m^4/s^3)
39	U_0	Ventilation velocity (m/s)
40	W_i	Velocity of the light flow at the source (m/s)
41	$U_{0,cr}$	Critical velocity (m/s)
42	φ	Tunnel blockage ratio
43	Rc	Critical velocity ratio
44	Re	Reynolds number
45	Γ	Plume Richardson number
46	X	Volume fraction

- 47 α Plume entrainment coefficient
48 C_f Dimensionless pressure coefficient
49 N_{PB} Number of pairs of blocks

50 **Subscripts**

- 51 $_0$ Property of the ambient condition
52 $_i$ Property of plume at the source
53 $_{he}$ Helium Properties

54 **Acronyms/ Abbreviations**

- 55 HRR Heat Release Rate
56 CFD Computational Fluid Dynamics
57 HGVs Heavy Goods Vehicles

58 **1. INTRODUCTION**

59 After the recent violent fires in road tunnels, such as the tragic fire that occurred in the Mont-Blanc tunnel between France
60 and Italy (1999, 39 dead), road tunnel safety has become a national and international issue. In France, since 1999, legislation
61 and regulations concerning the construction and operation of road tunnels have therefore been revised with a view to
62 improving safety. Recently, many studies have been conducted on tunnel fires, either in large-scale tunnel tests or in small-
63 scale thermal and densimetric models. Most of these studies concerned the control of smoke flow in the tunnel fires [1-7], the
64 evaluation of the critical velocity and smoke back-layering flow length [8-15], the determination of the power or the heat
65 release rate (HRR) of the fire inside road tunnels [16-21] and the aerodynamics of buoyant releases within a longitudinally
66 ventilated tunnel [6,22-25].

67 In the instance of a fire in a tunnel, smoke control is often the most important part of emergency planning. Ventilation
68 systems are one of the main protective measures to be adopted to prevent the spread of smoke upstream of the fire. They
69 allow tunnel users to ensure their own safety in reaching the refuges and provide better access to fight the fire. If the
70 ventilation velocity is low, the smoke produced by the fire may move upstream of the fire. This phenomenon is called ‘back-
71 layering’ and appears when the ventilation velocity is lower than the ‘critical velocity’ [26], which is defined as the minimum
72 ventilation velocity able to ensure all the combustion products remain downstream of the fire source in the tunnel.

73 Other than the heat release rate, many parameters are involved in the determination of the critical velocity, including heat
74 transfer processes [27-28], the tunnel geometry [1,7,11], the positions of the fans and the size of the fire [10,14]. Despite the
75 evident complexity of the physical system, the values of the critical velocities, against the HRR, can be controlled using
76 different strategies. One approach is that of using fixed solid barriers at the tunnel ceiling, which can prevent the spread of
77 fire and smoke upstream of the source, even for low ventilation velocities. In other words, by combining this strategy with
78 the longitudinal ventilation, the local longitudinal velocity increases in the tunnel cross-section area where the barrier is
79 installed. Therefore, a slower ventilation flow, compared to that in a empty tunnel, would be sufficient to prevent smoke from
80 spreading upstream of the fire. This strategy could be then effective in improving the safety of people and firefighters
81 upstream of the fire, since a large proportion of the smoke should be blocked near the ceiling.

82 Öttl et al. [29] tested a new system in the 5400 m long Katschberg tunnel (Austria), which consists of a new developed
83 synthetic material in the form of curtains. Their experiments revealed that the new system is effective in controlling the
84 smoke propagation at low longitudinal air velocity. A systematic investigation on the use of flexible devices for controlling
85 smoke and fire propagation in road tunnels was carried out by Bettelini and Rigert [30-31]. Their numerical results show that
86 flexible smoke curtains in longitudinally ventilated road tunnels allows the critical velocity to be reduced. They concluded
87 that this application offers important benefits in terms of controlling smoke. The effect of fixed smoke barriers on the
88 evacuation environment in road tunnel fires with natural ventilation was investigated by Seike et al. [32] using CFD
89 simulation. Their results show that smoke barriers help stop the propagation of the smoke and improve safety in tunnel fires.

90 In the perspective of evaluating the role of the blocking effect induced by barriers at the tunnel ceiling, it is also important to
91 consider the blocking effect induced by the presence of vehicles within the tunnel. In fact, the size and density of these
92 vehicles affect the longitudinal ventilation flow and therefore the dependence of the critical velocity on the heat release rates
93 (HRR). To date, several authors have studied the effects of vehicle blockages on smoke propagation upstream of fire and on
94 critical velocities in longitudinally ventilated tunnels. An initial study on the effects of vehicular blockages on critical
95 velocities was performed by Oka and Atkinson [3] who placed propane gas burners above solid blocks of broken vehicles in
96 reduced scale experiments. They concluded that solid blockages near the fire result in a reduction of the critical velocity. Lee
97 and Tsai [33] conducted small-scale experiments and numerical simulations considering three vehicles types in different
98 arrays, positioned upstream of the fires. Fires were located first on the tunnel centre line and then downstream of vehicle
99 obstructions. They found that the critical velocity decreased due to vehicular obstruction when the ventilation flow reached
100 fires directly, with a reduction ratio approximately equal to the vehicle blockage ratio. On the contrary, they showed that the

101 critical velocity increased when the vehicle obstructions did not allow the ventilation flow to directly reach the fires. These
102 general tendencies were then further confirmed by Tang et al. [34], Rojas Alva et al. [35] and Jiang [36]. Tang et al. [34],
103 who conducted experiments by placing a block upstream of a porous burner source on the centerline of the tunnel and
104 varying the relative distance between the block and fire source. Rojas Alva et al. [35] conducted an experimental study, in a
105 small-scale tunnel model in which the buoyant plume is modelled with an air/helium mixture, using three sizes of vehicular
106 obstacles and considering different arrays and various positions of the fire source along the tunnel width. Jiang [36] simulated
107 the fire source by means of a densimetric plume and considered different configurations, so that the buoyant source was
108 placed downstream either directly behind the vehicles or behind the spacing between the vehicles. He further showed that the
109 critical velocity is affected only by the block located close to the fire source, while the effect of the other blocks located
110 further upstream is negligible. Besides that, Gannouni and Maad [37] performed numerical simulations of fires in a
111 longitudinal ventilation tunnel to study the effect of the blockage on the critical velocity and the backflow length by varying
112 the distance between the bottom of the obstacle and the tunnel floor. Their results shows that the reduction in the critical
113 velocity is slightly higher with increasing distance between the bottom of the obstacle and the tunnel floor. Based small-scale
114 experimental results, Zhang et al. [38] proposed a physical model to predict the length of the smoke back-layering under the
115 blockage effect of metro train in subway tunnel.

116 The aim of this work is to analyse experimentally the effects of solid barriers placed at the tunnel ceiling on the propagation
117 of smoke in the instance of a fire within longitudinally ventilated tunnels. In the experiments, the hot smokes are simulated
118 by releases of light fluid, which have been shown [27] to induce ventilation conditions that are similar to those induced by the
119 presence of a fire (provided that its flames do not exceed the tunnel half height).

120 We consider two types of barriers: small fixed barriers with a height equal to $H/10$ (H is the tunnel height) and larger but
121 mobile barriers with a height equal to $H/4$ and $H/3$. Unlike fixed ones, mobile barriers are deployed only in the event of fire
122 and placed upstream of the source in longitudinal ventilation.

123 This work is split into two parts. In the first part, we evaluate the effects of barriers on the spread of smoke upstream of the
124 fire source in the tunnel. In the second part, we examine the effects of these barriers on pressure drops. In both parts, we carry
125 out the study, first in an empty tunnel (without vehicles), then in a tunnel with vehicles placed upstream of the source.
126 Vehicles are modelled by blocks of three different sizes; small, medium and large blocks which could represent
127 approximately small cars, lorries and Heavy Goods Vehicles in real tunnels, respectively. Conclusions are drawn regarding
128 the effectiveness of the barriers to control the propagation of smoke by evaluating the results of both parts.

129 2. EXPERIMENTAL SET UP

130 The experiments have been performed with a densimetric reduced scale model of a tunnel (see Fig. 1), in which the fire-
131 induced smoke is represented by a continuous release of a light fluid, a mixture of air and helium. The tunnel model, whose
132 scale can be considered in the range between 1/25 and 1/30 of a real scale tunnel, is the LMFA (Laboratoire de Mécanique
133 des Fluides et d'Acoustique) laboratory, consists of a 8.4 m long channel with a rectangular cross-section of 0.36 m wide and
134 0.18 m high. The rear wall is made of 19 mm thick chipboard panels and the side wall is made of toughened glass which
135 allows visualisation of the flow coming from the source. The floor and ceiling are made of 19 mm panels Medium Density
136 Fiberboard (MDF). To induce a longitudinal air flow, the tunnel is equipped with an extraction fan at its end, which can
137 generate a varied airflow between 20 and 355 m³/h. A potentiometer is wired to this fan to control its speed. The ventilation
138 velocity inside the tunnel is measured by means of a Pitot tube placed within an airflow cone at the tunnel inlet, which has
139 been calibrated before being placed in the tunnel. The buoyant source is modelled by a densimetric plume [27], mixture of air
140 and helium. The flow rates of air and helium are controlled independently and measured by two flow metres. The light plume
141 is released from a circular source with a diameter of $D_1 = 0.1$ m. The top surface of the source is set flush with the floor on the
142 axis of the tunnel, and placed at a distance of 4.55 m from the tunnel inlet. The mixture of air and helium is seeded with oil
143 particles before being injected in the plenum. These particles or tracers diffuse the intense light of the laser sheet emitted by a

144 lens placed at the inlet box of the tunnel. This technique reveals a two-dimensional slice of the flow in the area of interest
 145 inside the tunnel. The air flow that is used for seeding is controlled by a flow meter. This is taken into account and added to
 146 the mixing flow of air and helium to determine the conditions at the source, i.e. density and velocity. Compared to the
 147 mixture of air-helium flow, the air flow used for seeding is very low, which implies that the mass of oil added to seed does
 148 not affect the density of the mixture.

149 The plume density at the source (ρ_i) is:

$$\rho_i = X_0\rho_0 + X_{he}\rho_{he} \quad 1$$

150 where ρ_0 is the density of air, ρ_{he} is the density of helium and X_0 , X_{he} , are the volume fractions of air and helium,
 151 respectively given by:

$$X_0 = \frac{q_0}{q_i} = \frac{\rho_i - \rho_{he}}{\rho_0 - \rho_{he}}, \quad X_{he} = \frac{q_{he}}{q_i} = \frac{\rho_0 - \rho_i}{\rho_0 - \rho_{he}} \quad 2$$

152 where $q_i = q_{he} + q_0$ the volume flow defined by the sum of the two volume flows of air (q_0) and helium (q_{he}).

153 We have produced a variety of light fluid releases, with different buoyancy flux values $B_i = gq_i \frac{\rho_0 - \rho_i}{\rho_0}$ (g is the gravitational
 154 acceleration) in the range $0.0139 < B_i \text{ (m}^4/\text{s}^3) < 0.062$. These releases are characterised by a varying plume Richardson
 155 number larger than unity. The latter is defined as:

$$\Gamma_i = \frac{5}{16\alpha} \frac{(\rho_0 - \rho_i)g}{\rho_0} \frac{D_i}{W_i^2} \quad 3$$

156 where $W_i = \frac{4q_i}{\pi D_i^2}$ is the velocity at the source and $\alpha = 0.12$ is a reference entrainment coefficient [25]. The value of the plume
 157 Richardson number allows for a classification of different plume typology [24-25]. A plume with $\Gamma_i < 1$ is referred to a
 158 ‘forced’ plume, whose dynamics are momentum dominated, whereas a plume with $\Gamma_i > 1$, whose dynamics are dominated by
 159 the role of buoyancy, is said to be ‘lazy’. The condition $\Gamma_i = 1$ corresponds instead to a ‘pure plume’, in which buoyancy and
 160 momentum effects are in balance. As shown by Jiang et al. [27] the back flow of light fluid at the ceiling induced by a lazy
 161 plume accurately reproduces the behaviour of hot smokes produced by a fire with flames whose length does not exceed the
 162 tunnel half height. The experimental tests were therefore carried out for lazy plumes, where $\Gamma_i = 2, 4, 6, 8$ and 10 . The density
 163 ratio was fixed and equal to $\rho_i/\rho_0 = 0.7$. As shown by Salizzoni et al. [28], its variations do not affect the dynamics of
 164 buoyancy generated releases.

165 An initial investigation concerns the influence of the longitudinal ventilation velocities on the buoyant fluid propagation
 166 inside the tunnel without barriers. The measurements consist of determining the length of back-layering flow inside the
 167 tunnel, by means of flow visualisation, against the longitudinal airflow. For each value of the plume Richardson number, the
 168 critical velocities are reached by increasing the ventilation velocities until the back-layering flow disappears.

169 To investigate the effect of barriers, two types of barriers were tested, small and large barriers. The barriers are solid and their
 170 width is equal to the tunnel width.

171 The small barriers have a height equal to 1/10 the tunnel height. They are fixed at the tunnel ceiling over a distance that
 172 ranges from 2.4 to 5.4 meters (i.e. 2.15 m upstream of the source and 0.75 m in downstream of the source). The barriers are
 173 placed so that one of these is fixed just upstream of the source. Two configurations are tested, in the first, all the barriers are
 174 placed so that $S = H$ (Fig. 1a) and in the second $S = 2H$ (Fig. 1b), where S is the distance between each two adjacent barriers.
 175 For the large barriers only one barrier will be fixed to the tunnel ceiling, we choose two heights $H/4$ and $H/3$. For each case,
 176 the barrier is initially placed just upstream of the source (Fig. 1d) and then placed at a distance equal to the tunnel height
 177 upstream of the source, i.e. $d = H$ (Fig. 1c).

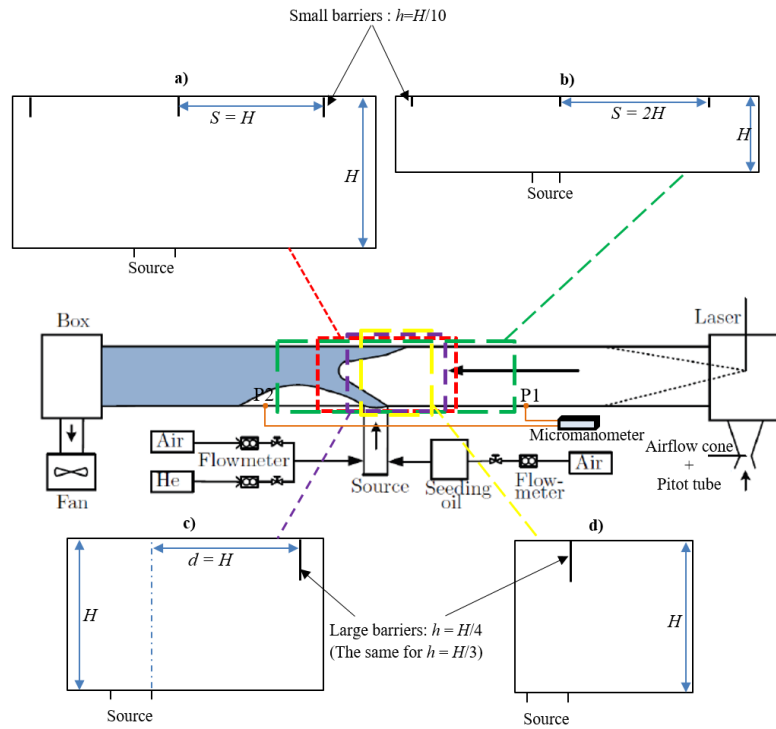


Fig. 1. Schematic of the experimental setup with barriers fixed at the tunnel ceiling. h is the height of barrier, d is the distance between the source and the large barrier and S is the distance between each two adjacent small barriers.

178 The flow was illuminated by a laser sheet emitted by a lens installed at the tunnel inlet. In the laser sheet technique, the
 179 buoyant mixture is seeded with nebulised oil particles. A thin sheet of light is then introduced in the same direction of flow,
 180 illuminating the seed particles. The image of the flow thus illuminated is then recorded using a camera. By adjusting the fan
 181 power, we can determine the critical velocities and the back-layering lengths of each tested longitudinal ventilation velocity.
 182 Typical critical ventilation conditions for a tunnel with the largest barrier ($H/3$) and tunnel without barriers are shown in **Fig.**
 183 **2b** and **Fig. 2a**, respectively. Both flow visualisations are taken with the same source conditions, but at different critical
 184 conditions. The critical velocity, $U_{0,cr}$, measured in the case without barrier is equal to 0.25 m/s, while that measured in the
 185 tunnel with barrier is equal to 0.14 m/s. This means that the large barrier ($H/3$) can prevent the smoke back-layer at a reduced
 186 critical ventilation velocity. In this case: $U_{0,cr \text{ with barrier}} \approx 0.56 * U_{0,cr \text{ without barrier}}$, which means that the reduction of the
 187 critical velocity is about 44%.

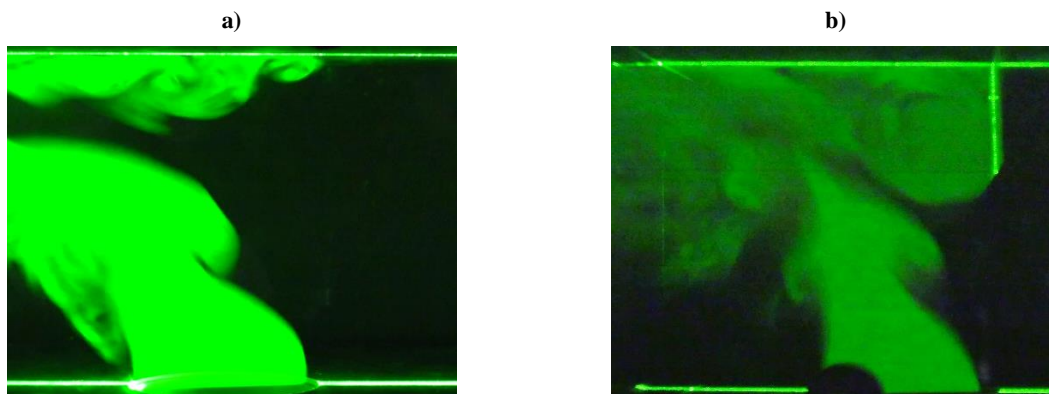


Fig. 2. Critical ventilation condition with $\Gamma_i = 2$. a) Tunnel without barriers ($U_{0,cr} = 0.256$ m/s). b) Tunnel with a largest barrier of height $H/3$ placed just upstream of the source ($U_{0,cr} = 0.143$ m/s).

188 Note that the interaction between the longitudinal flow and the smoke plume exhibits fluctuations implying uncertainties in
 189 the visual estimates of smoke back-layering length. These uncertainties are estimated to equal approximately 10% of the
 190 value of measured back-layer length.

191 In order to simulate the effect of vehicles on the smoke propagation, we examined three kinds of cubic blocks: cubes with
 192 dimensions 0.05 m (block1), 0.08 m (block2) and 0.12 m (block3). Blocks 1, 2 and 3 may represent approximately small
 193 vehicles, lorries and Heavy Goods Vehicles (HGVs), respectively, in the real tunnels. **Fig. 3** shows a schematic diagram of
 194 the top view and the side view in the tunnel cross-section of block locations in the experiment. For each set of blocks, we
 195 consider only one configuration in which two rows of blocks were placed at the sides upstream of the source. The aim is to
 196 represent the case of unidirectional tunnels which might be used for two-lane traffic.

197 In order to evaluate the effect of traffic congestion in the tunnels, we do the experiments with a variable number of pairs of
 198 blocks ranging from one to six for large blocks, from one to seven for medium blocks and from one to eight for small blocks.
 199 In these experiments, the Richardson number at the source was set to 2 and the density ratio was set to 0.7.

200 In order to assess the impact of the distance between the source and the position of the blocks, we first placed all the blocks
 201 in such a way that the last pair is positioned just upstream of the source, then for each successive test the pair of blocks
 202 closest to the source is removed. The distance between each pair of blocks remains constant along the two lanes and is equal
 203 to $2H$.

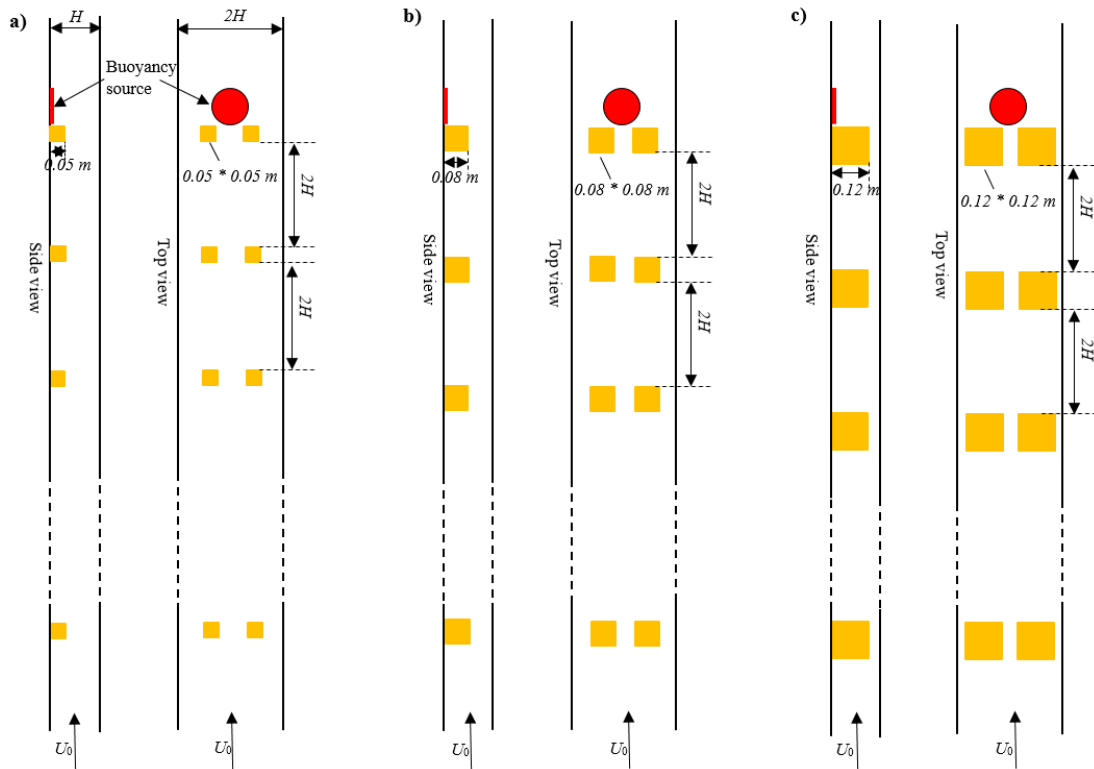


Fig. 3. The block locations in the experiment. a) Block1: 0.05 m^3 . b) Block2: 0.08 m^3 . c) Block3: 0.12 m^3 . We keep the same configuration of blocks in the case of a tunnel with barriers fixed to the ceiling.

204 We performed experiments with and without barriers, with the configurations sketched in **Fig. 1**. However, for large barriers
 205 only the case where the barrier is placed just upstream of the source is presented as we only want to study their effects on the
 206 critical velocities in the presence of vehicular blockage. The barriers also represent a blockage entailing a reduction of the
 207 tunnel cross-section (see **Fig. 4b**).

208 In what follows both the effect of barriers and blocks will be considered as a function of their blockage ratio, defined as the
 209 ratio between the cross section occupied by the obstacle and the cross section of the tunnel. This ratio can be linked to an
 210 equivalent increase ratio of the local critical velocity. To enlighten this we define $U_{0,1}$, A_1 , the flow velocities and tunnel cross

211 sectional areas at position (1), i.e. away from the block and $U_{0,2}$, A_2 , the flow velocities and tunnel cross sectional areas at
 212 position (2), where the block is placed (see **Fig. 4a**). The tunnel blockage rate is given by $\varphi = (A_1 - A_2)/A_1$. Since the volume
 213 flow conservation implies that: $U_{0,1} * A_1 = U_{0,2} * A_2$, we can evaluate an equivalent ratio between the local critical velocity $U_{0,2}$
 214 and that in the empty tunnel $U_{0,1}$ as:

$$U_{0,2} / U_{0,1} = A_2 / A_1 \quad 4$$

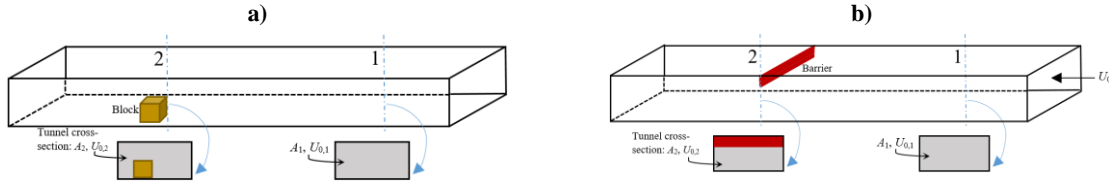


Fig. 4. Schematic representations of obstacles placed in tunnel of rectangular cross-section. Obstacle is represented by a block in figure (a) and by a barrier in figure (b). A_1 , $U_{0,1}$, A_2 , $U_{0,2}$ are the relative flow velocities and tunnel cross-sectional area (in grey).

215 In **Table 1**, we summarise the obstacle-induced blocking rates of all the possible combinations of blocks and barriers placed
 216 on the same cross-section.

	without barriers	Barrier with height $H/10$	Barrier with height $H/4$	Barrier with height $H/3$
Without blocks	00%	10%	25%	33%
Pair of block1	08%	18%	33%	41%
Pair of block2	20%	30%	45%	53%
Pair of block3	44%	54%	69%	77%

Table 1. Blockage rates induced by blocks and barriers

217 Note that the blocking rates induced by the presence, on the same cross section, of larger blocks (block3) and large barriers
 218 ($H/4$ or $H/3$), i.e. 69% and 77%, respectively, are significantly higher compared to all others. Therefore, we placed the last
 219 pair of block3 slightly behind the large barrier at a distance of about one centimetre. The aim is to both slightly reduce the
 220 blockage ratio and potentially avoid contact between the barrier and the blocks.

221 3. EFFECT ON BACKLAYERING AND CRITICAL VELOCITY

222 Our aim is to clarify the effect of solid barriers placed at the tunnel ceiling on the propagation of smoke upstream of the
 223 source in a longitudinally ventilated tunnel. In particular, two aspects are studied:

- 224 - Effects of barriers on the extension of smoke back-layer according to source conditions and ventilation flows.
- 225 - Effects of barriers on the critical velocity according to the source conditions.

226 The study of these parameters is first done in the tunnel without blocks. The objective is to compare the results obtained in
 227 the two tunnel configurations with and without barriers and to determine the reduction of the critical velocity due to each type
 228 of barrier. The study is then extended to include the effects of blocks to assess the influence of vehicular traffic on critical
 229 ventilation velocities in the tunnel with and without barriers.

230 3.1 TUNNEL WITHOUT BLOCKS

231 Experimental results of the effects of barriers on smoke propagation inside the tunnel with and without barriers are presented
 232 hereafter. First, we evaluate the effects of barriers on the smoke back-layering lengths. Then, we conduct more experiments
 233 to study their effects on critical ventilation velocities.

234 3.1.1 Smoke back-layering flow length

235 Several experimental measurements were performed to evaluate the smoke back-layering flow length against the ventilation
 236 velocity. The experiments are carried out, both in the tunnel without barriers and in the tunnel with different barriers, under
 237 the same source conditions (i.e. $\Gamma_i=2$ and $\rho_i/\rho_0=0.7$).

238 **Fig. 5** and **Fig. 6** show a plot of the dimensionless back-layering flow length, L/H , against the velocity ratio $U_0/U_{0,cr}$. $U_{0,cr}$
 239 refers to the ‘critical velocity’ measured in the empty tunnel (tunnel without barriers). The ratio $U_0/U_{0,cr}$ is the parameter that
 240 reveals the effects of the barriers on the smoke propagation. **Fig. 5** compares the results obtained in the empty tunnel and in
 241 the tunnel with small barriers of both configurations $S = H$ and $S = 2H$. The results show that the critical velocity reduction
 242 ratio by the effect of the barriers (i.e. the minimum ratio that corresponds to a back-layer length = 0) is improved for the
 243 instant when $S = 2H$. In this case, the barrier located just upstream of the source prevents the smoke back-layering flow for
 244 any velocity $U_0 > 0.83*U_{0,cr}$. Meanwhile in the case when $S = H$, the first barrier placed just upstream of the source prevents
 245 the return of smoke for any velocity ratio $U_0/U_{0,cr} > 0.91$. Therefore, a different reduction ratio between the two
 246 configurations explains the importance attached to the distance S fixed between each two adjacent barriers. In the case where
 247 $S = H$, the reduction of the critical velocity is low because the first barrier located downstream of the source creates an
 248 obstruction for the smoke which forces it to go upstream. This obstruction has less influence when the distance S is large. In
 249 such a case, the barrier is located far from the impingement region of the buoyant releases and the smoke flows downstream
 250 of the source without being blocked. Consequently, a lower ventilation velocity, compared to that when $S = H$, is needed to
 251 prevent smoke from flowing upstream of the source. However, for velocity less than the threshold value specified above (i.e.
 252 $U_0 < 0.83*U_{0,cr}$ when $S = 2H$ and $U_0 < 0.91*U_{0,cr}$ when $S = H$), the smoke back layer can be seen even with barriers in place,
 253 although the back layer length is reduced compared to the case with no barriers. This is expected because the barriers placed
 254 further upstream of the source prevent the back-layering flow at low ventilation velocities.

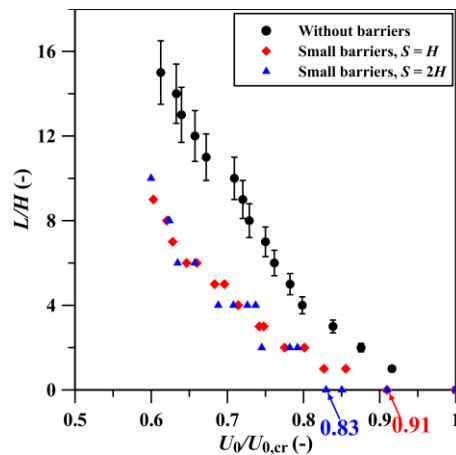


Fig. 5. Smoke dimensionless back-layering length, L/H , measured in the tunnel with and without small barriers against the ratio of longitudinal ventilation velocity to the critical velocity $U_0 / U_{0,cr}$ ($U_{0,cr}$ is the critical velocity in the tunnel without barriers).

255 Results for the tunnel with a large barrier ($H/4$ and $H/3$) are shown in **Fig. 6** and compared to those obtained in the empty
 256 tunnel. **Fig. 6a** shows the result for the case when the large barrier is placed just upstream of the source and **Fig. 6b** shows
 257 the result when the barrier is fixed at a distance H upstream of the source. In both cases, the results show that the large barrier
 258 prevents the smoke from flowing upstream of the source for any ventilation velocity greater than or equal to $0.67*U_{0,cr}$ for
 259 barrier height $H/4$ and $0.56*U_{0,cr}$ for barrier height $H/3$. This means that the distance between the barrier and the source
 260 position does not affect the reduction ratio, i.e. the effectiveness of the barrier is not dependent on its distance from the
 261 source. This is important because, in practice, it is impossible to predict where a fire will occur inside the tunnel and,
 262 therefore, each barrier should be able to cover a large area whatever its location in the tunnel. However, for any velocity U_0
 263 less than $0.67*U_{0,cr}$ for $h = H/4$ and $0.56*U_{0,cr}$ for $h = H/3$, the barrier can not stop the propagation of the smoke upstream of

264 the source, but it does nevertheless play a significant role in minimising the back layer length. As shown in **Fig. 6a** and **Fig.**
 265 **6b**, the back-layer length in the tunnel with a large barrier remains lower than that in the tunnel without the barrier.
 266 Finally, by comparing all the previous results, we can conclude that the effectiveness of barriers increases with increasing
 267 height.

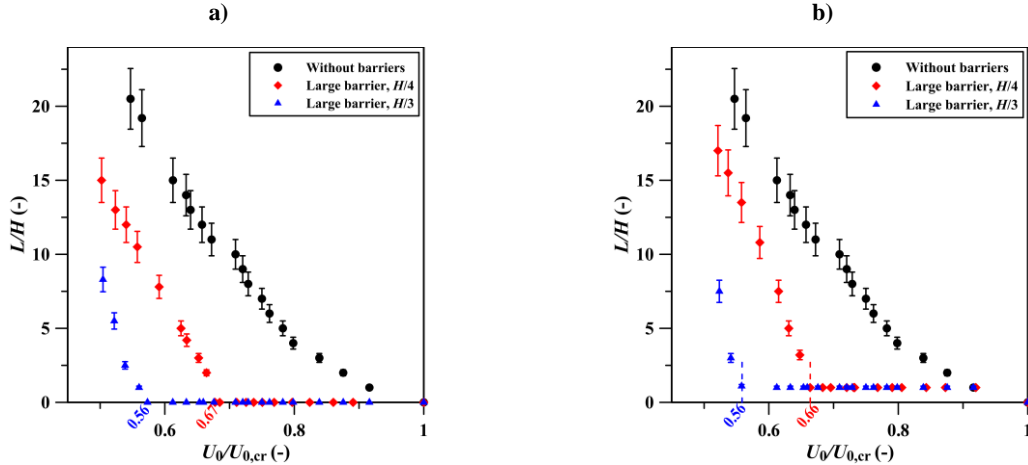


Fig. 6. Smoke dimensionless back-layering length, L/H , measured in the tunnel with and without large barriers against the ratio of longitudinal ventilation velocity to the critical velocity $U_0 / U_{0,cr}$. a) The barrier is placed just upstream of the source. b) The barrier is placed at a distance H upstream of the source.

268 3.1.2 Critical longitudinal ventilation velocities

269 More experiments were conducted to study the effect of barriers on the critical velocity $U_{0,cr}$. The critical velocity in the
 270 empty tunnel and in the tunnel with barriers is defined as:

271 - The minimum longitudinal velocity needed to prevent the back-layering flow upstream of the buoyant source in
 272 the tunnel with no barriers.

273 - The minimum longitudinal velocity for which the barrier placed just upstream of the source prevents the back-layer
 274 flow in the tunnel with barriers.

275 **Fig. 7a** and **Fig. 7b** show the dependence of the critical ventilation velocity $U_{0,cr}$ on the buoyancy flux B_i and the dependence
 276 of the dimensionless critical velocity $U_{0,cr}/W_i$ on the plume Richardson number Γ_i , respectively. As expected, for all cases,
 277 $U_{0,cr}$ increases with the increasing of the buoyancy flux B_i and dimensionless critical velocity $U_{0,cr}/W_i$ increases with the
 278 plume Richardson number Γ_i . As shown by Le Clanche et al. [23], these dependences can be conveniently fitted by power
 279 laws in the form $U_{0,cr} = aB_i^{1/3}$ and $\frac{U_{0,cr}}{W_i} = b\Gamma_i^{1/3}$. Note however that the 1/3 power laws are expected to fit data for releases
 280 with $\Gamma_i \gg 1$ and that therefore we would not expect these to hold for releases with Γ_i of order one [39]. This explains why
 281 values with lower Γ_i (corresponding to releases with highest B_i) do not fit well the regression curve. The constants 'a' and
 282 'b', obtained by a best-fit to the experimental data, both decrease when the size of the barriers increases (passing from an
 283 empty tunnel to a tunnel with the largest barrier, this constant is reduced by forty five percent). Note that the values of the
 284 constants $a = 0.96$ and $b = 0.36$ obtained in the empty tunnel (tunnel without barriers) are very similar to those determined by
 285 Le Clanche [23] in similar experiments in another experimental set-up.

a)

b)

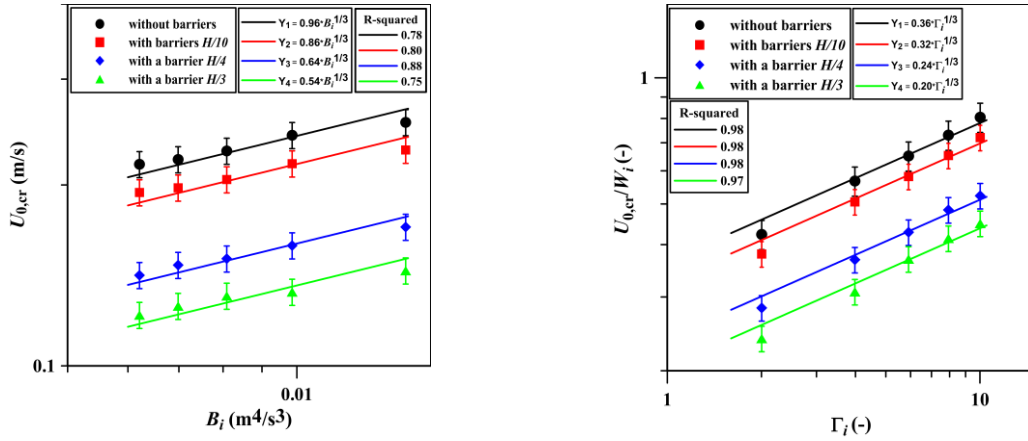


Fig. 7. a) Dependence of the critical velocity $U_{0,cr}$ on the buoyancy flow. b) Dependence of non-dimensional critical velocity on the plume Richardson number. All data are fitted with a power-law of the form $aX^{1/3}$. The estimated error rate of the experimental data is 5%. R-squared is the coefficient of determination for regression curves. The results for the small barriers presented here concern those with the configuration $S = H$.

286 In order to evaluate the effect of the barriers on the critical velocities, we have calculated the ratio between the critical
 287 velocities of a tunnel with barriers and those of a tunnel without barriers:

$$Rc = \frac{U_{0,cr} \text{ with barriers}}{U_{0,cr} \text{ without barriers}} \quad 5$$

288 The results, presented in **Fig. 8**, shows that the critical velocity ratio is almost independent of the plume Richardson number,
 289 i.e. this ratio is independent of the dynamical conditions at the buoyancy source. However, the ratio does depend on the
 290 barrier height, it decreases when the barrier height is large and vice versa. **Fig. 8** shows that the barriers with heights, $H/10$,
 291 $H/4$ and $H/3$ reduce 10%, 34% and 44% of critical velocities measured in the empty tunnel, respectively. In addition, the
 292 reduction ratio (i.e. $1 - Rc$) for $U_{0,cr}$ is approximately equal the tunnel blockage ratio (φ) induced by the different barriers
 293 (presented in **Table 1**: 10% for the barrier height $H/10$, 25% for the barrier height $H/4$ and 33% for the barrier height $H/3$).
 294 This is simply a consequence of the Venturi effect induced by the presence of barriers, i.e. an acceleration of the flow due to
 295 a reduction of the tunnel section, according to basic mass-conservation principle.

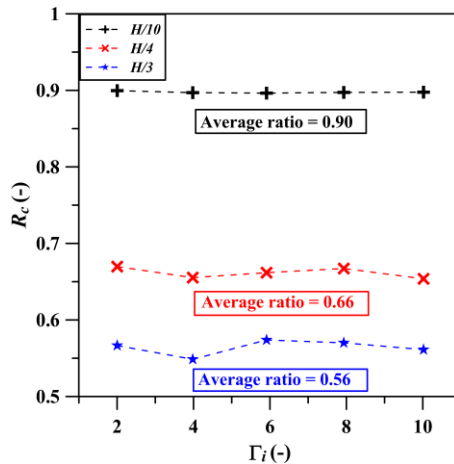


Fig. 8. The velocity ratio given by the critical velocity in the tunnel with barriers to the critical velocity in the empty tunnel against the plume Richardson number Γ_i .

296 3.2 TUNNEL WITH BLOCKS

297 The experimental data regarding the effects of obstacle blocking on critical velocities in case of fire in a longitudinal
 298 ventilated tunnel are plotted in **Fig. 9**, showing the results of all the possible combinations between the barriers and the
 299 blocks in a tabular form (presenting the three blocks in three rows and the four barrier configurations in four columns). The

300 data are plotted as the critical velocity ratio, R_c , (given by Eq. 5) against the number of pairs of blocks, N_{PB} (because there
 301 are two rows of blocks).

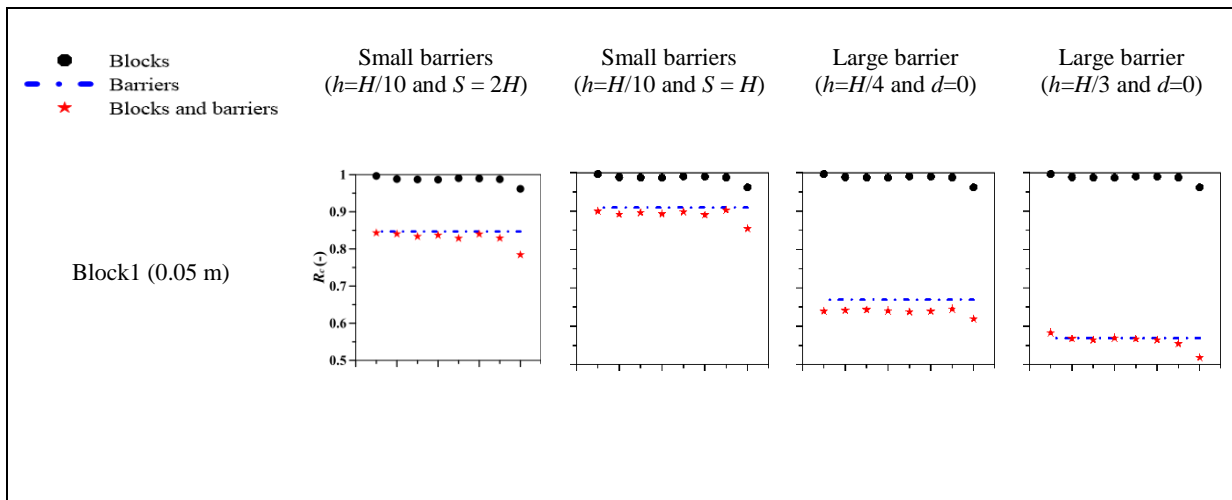
302 In Fig. 9 the black, blue and red symbols show the results obtained in the tunnel with blocks, with barriers and with set of
 303 blocks and barriers, respectively. The effects of barriers on critical velocities in empty tunnel have already been analysed in
 304 section 3.1.2 and presented here for comparison purposes. Now, we shall particularly focus on the effects of blocks in tunnels
 305 with and without barriers (i.e. the two series in black and red).

306 3.2.1 Effect of blocks in tunnel with no barriers

307 Fig. 9 shows that the influence of the blocks on the critical velocity varies according to the size of the blocks and the
 308 blockage-source distance, in agreement with what was observed by Jiang [36]. For small blocks (i.e. Block1), the results
 309 show that only the pair of blocks located just upstream of the source can slightly modify the value of the critical velocity,
 310 while the effect of the other blocks placed further upstream is negligible. The reduction in critical velocity due to the pair of
 311 small blocks located close to the source is equal to about 5%. This value is approximately equal to half of the blocking rate
 312 induced by the blocks. Regarding Block2 and Block3, the data show that when the distance between the blockage and the
 313 source decreases, the velocity ratio first decreases progressively, then suddenly drops once the source-blocks distance is zero.
 314 As a result, the critical velocity reductions associated with placing a pair of block2 and block3 directly behind the source are
 315 about 16% and 39% respectively. These values are close to the blocking rates induced by the same blocks (see Table 1). On
 316 the other hand, we can see that the reduction of the critical velocity due to the blocks situated further upstream of the source
 317 does not exceed 9% for both block2 and block3.

318 3.2.2 Effects of blocks in tunnel with barriers

319 The comparison between the results obtained in the case of a tunnel with barriers and those obtained in the case of a tunnel
 320 with blocks and barriers allows us to make two conclusions concerning the effects of source-blocks distance on the
 321 ventilation critical velocity. The first conclusion can be made from the case where the blocks are placed further upstream of
 322 the source. In this instance Fig. 9 shows a clear correlation between the blue and red curves in almost all tunnel
 323 configurations, excluding a few points with a lower value of R_c for when both blocks and barriers are present opposed to just
 324 barriers. This means that the blocks placed further upstream of the source have no effect on the critical velocity and the
 325 reduction observed in the series in red is only induced by the presence of the barriers. The second conclusion can be drawn
 326 from the case where the last pair of blocks is positioned close to the source. In this instance, we clearly see a drop in the
 327 values of the velocity ratio R_c appearing on all the curves of Fig. 9. This indicates that the critical velocity is only influenced
 328 by the blocks located just upstream of the source. Furthermore, it is clear from this figure that the decrease of R_c depends on
 329 both the size of the barriers and the size of the blocks; the reduction is high with large barriers or with large blocks and
 330 exceedingly high with the combination of both large barriers and large blocks.



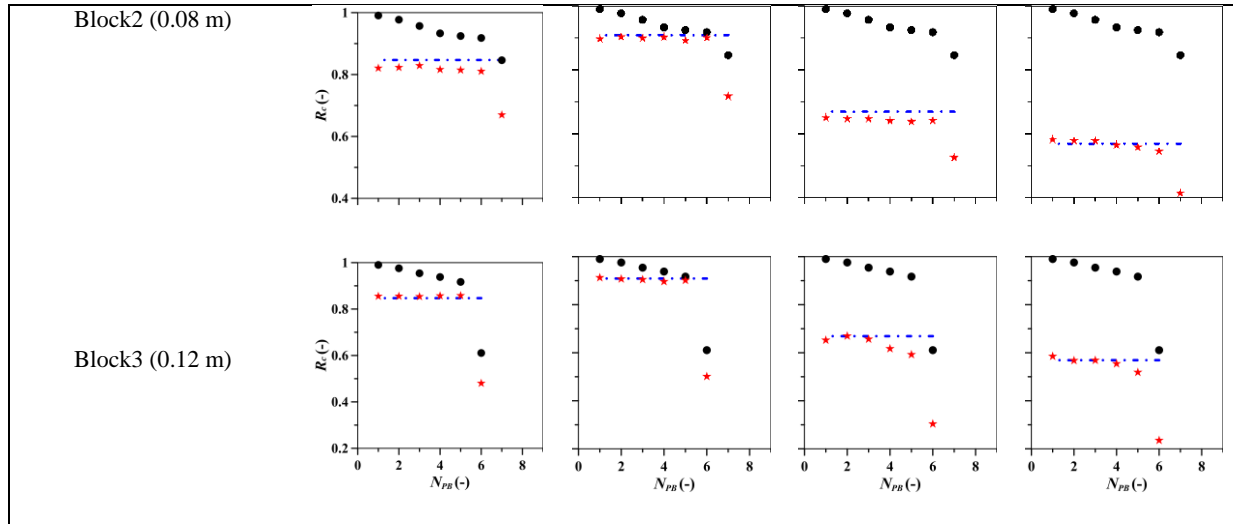


Fig. 9. The velocity ratio Rc -given by the critical velocity in the tunnel with obstacles to the critical velocity in the empty tunnel- against the number of pairs of blocks N_{PB} . $D_i = 0.1$ m, $\Gamma_i = 2$ and $\rho_i/\rho_0 = 0.7$.

331 **Table 2** summarises the rates of velocity reduction due to the location on the same cross section of a pair of blocks and a
 332 barrier upstream near the source.

	Small barriers ($h=H/10$ and $S = 2H$)	Small barriers ($h=H/10$ and $S = H$)	Large barrier ($h=H/4$ and $d=0$)	Large barrier ($h=H/3$ and $d=0$)
Pair of block1	22%	15%	38%	48%
Pair of block2	33%	28%	48%	59%
Pair of block3	52%	50%	70%	77%

Table 2. Velocity reduction rates induced by both the pair of blocks and the barrier located on the same cross-section just upstream of the source.

333 The data for the reduction of the critical velocities ($1 - Rc$) due to blockage caused by barriers, blocks or both are collected
 334 and plotted in **Fig. 10** according to the corresponding tunnel blockage ratios (ϕ). Only results with obstacles located just
 335 upstream of the source are presented in this figure. By fitting the data with a linear regression, results suggest that the critical
 336 velocity reduction rate is proportional to the blockage ratio, i.e. $1 - Rc = \phi$. Using **Eq. 5**, this relationship can be written in
 337 the form:

$$\frac{U_{0,cr \text{ with blockage}}}{U_{0,cr \text{ without blockage}}} = 1 - \phi \quad 6$$

338 which is equivalent to **Eq. 4**, derived from the conservation principle of the volume flow. This means that when an obstacle is
 339 located near the source (provided it does not directly affect the longitudinal airflow that reaches the smoke plume), a lower
 340 ventilation flow is sufficient to force all the smoke downstream of the source, since the local ventilation velocity increases in
 341 proportion to the reduction of the tunnel cross section. Therefore, the reduction ratio of the critical velocity will be almost
 342 equal to the tunnel blockage ratio.

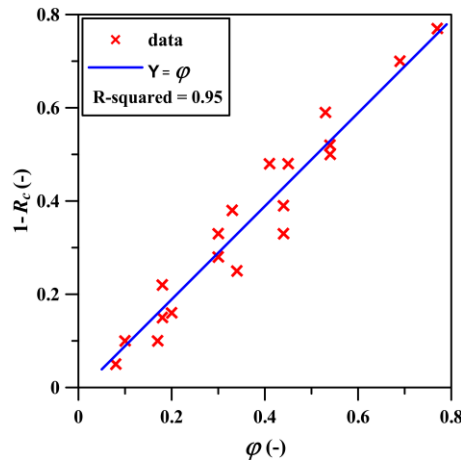


Fig. 10. Reduction of the critical velocities ($1 - R_c$) against the tunnel blockage ratios (ϕ) of obstacles (barrier, block, or both) located just upstream of the source.

343 However, when the distance between the blocks and the source is equal to or greater than twice the height of the tunnel, the
 344 reduction in the critical velocity is too low (**Fig. 9**). Therefore, to obtain a complete critical ventilation model considering the
 345 blockage and the source-blockage distance, additional tests are required (these should be performed by reducing the
 346 increasing distance between the source and the blocks).

347 4. EFFECT ON THE PRESSURE LOSSES ALONG THE TUNNEL

348 In the case of a tunnel without any blocks, we have seen that the barriers prevent the smoke back-layer up to a certain so-
 349 called critical velocity ratio, which depends mainly on the barrier height. On the other hand, in the presence of blocks inside
 350 the tunnel, the critical velocity was greatly affected by the size of blocks which are placed close to the source. However, the
 351 design and dimensioning of the ventilation systems installed in the tunnels are determined by the sum of the pressure losses
 352 created in the ventilation networks. Adding barriers or blocks in the tunnel induces an increase in pressure drops and
 353 potentially an increase in the capacity of machines to be installed. It is therefore essential to evaluate these additional pressure
 354 losses generated by the obstacles. For that purpose, an experimental study was carried out to first examine the effects of
 355 barriers on the pressure drop in a tunnel without any blocks, then the effects of vehicular blockage in the tunnel with and
 356 without barriers. The experiments on pressure losses were performed in the reduced-scale tunnel shown in **Fig. 1**, without
 357 releasing any buoyant fluid.

358 To study the effects of the barriers, we consider almost the same configurations presented previously and illustrated in **Fig. 1**.
 359 We focus on the effect of the number of small barriers fixed to the tunnel ceiling and the effect of barrier heights.

360 To analyse the effects of the vehicular blockages on the pressure drops, we perform the same experiments as those presented
 361 previously (see **Fig. 3**). By considering the same blocks placed on the tunnel floor in the same configuration as that shown in
 362 **Fig. 3** (except here the source of buoyancy is not considered). In that we focus mainly on the effect of the number of blocks
 363 placed in the tunnel and the effect of the block sizes.

364 The pressure difference was measured between two points, one upstream and the other downstream of the obstacle
 365 positioning area. The obstacle positioning area extends from 2.4 m to 5.4 m and the two points P1 and P2 are located at
 366 ground level of the tunnel (**Fig. 1**) at 2.1 m and 5.7 m from the inlet, separated by the distance $L_{1-2} = 3.6$ m. The
 367 measurements were performed using a highly-accurate measuring device (FCO510 Micromanometer [40]). The instrument
 368 contains a highly sensitive ultra-low-range differential pressure transducer with a resolution of up to 0.001 pascals. It is
 369 capable of making pressure difference measurements in the range of 2-20 mmH₂O with a measurement accuracy of $\pm 0.25\%$
 370 of reading between 10% of lowest range and full scale. The micromanometer retrieves the pressure difference every 0.3
 371 seconds and sends the values to the computer where they are averaged over 5 min using the software LabVIEW. This mean
 372 value corresponds to the mean pressure difference Δp .

373 As pressure differences are caused by the dynamic pressure, it is convenient to introduce a dimensionless pressure coefficient
 374 C_f defined as:

$$C_f = \frac{\Delta p / L_{1-2}}{\frac{1}{2} \rho_0 U_0^2 / \bar{D}} \quad 7$$

375 where \bar{D} is the hydraulic diameter of the tunnel defined as $\frac{2HW}{(H+W)}$, W is the width of the tunnel, H is the height of the tunnel,
 376 ρ_0 is the density of ambient air and U_0 is the longitudinal ventilation velocity.

377 **4.1 EFFECTS OF BARRIERS**

378 To investigate the effects of the barriers on pressure losses, we consider the three barriers having heights $H/10$, $H/4$ and $H/3$.
 379 In case of the small fixed barriers, i.e. $H/10$, we consider two different configurations, with a spacing between the barriers of
 380 $S = H$ and $S = 2H$. For the large barriers i.e. $H/4$ and $H/3$, a single barrier is fixed to the tunnel ceiling. **Fig. 11** shows the
 381 results concerning the dependence of dimensionless pressure coefficient, C_f , against the ratio, h/H , at a high Reynolds
 382 number ($Re > 17000$). The additional pressure loss produced in the tunnel as a result of the barriers is compared to that
 383 induced in the empty tunnel. The results show that:

- 384 - The coefficient of pressure loss increases with the increase in the number of obstacles: for small barriers, the
 385 pressure losses induced by the barriers in the configuration with a spacing $S = H$ is greater than those induced in the case with
 386 $S = 2H$.
- 387 - The pressure losses increase with increasing the barrier height: for large barriers, the pressure loss induced by the
 388 largest barrier ($H/3$) is higher than that induced by the barrier of the height $H/4$.
- 389 - The pressure losses created by the largest barrier ($H/3$) are slightly greater than those created by nineteen (19) small
 390 barriers (19 is the number of small barriers with the configuration $S = H$).

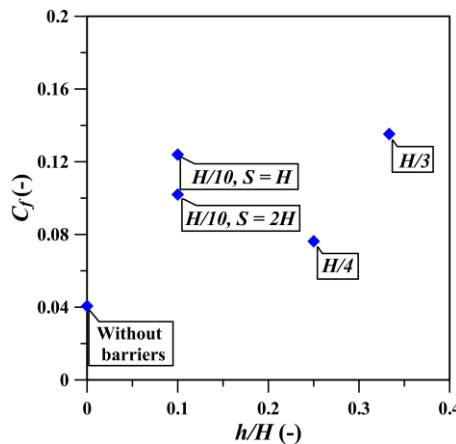


Fig. 11. Dimensionless pressure coefficient, C_f , against the dimensionless barrier height, h/H .

391 **4.2 EFFECTS OF VEHICULAR BLOCKAGE**

392 **Fig. 12** shows the results for the pressure drops due to the presence of the blocks in the tunnel for both cases with and without
 393 barriers against the number of pairs of blocks, N_{PB} . Taking the results in the tunnel without blocks as a reference case (i.e.
 394 curves in blue), we can classify two cases:

●	Blocks	Small barriers	Small barriers	Large barrier	Large barrier
—	Barriers	($h=H/10$ and $S=2H$)	($h=H/10$ and $S=H$)	($h=H/4$ and $d=0$)	($h=H/3$ and $d=0$)
*	Blocks and barriers				

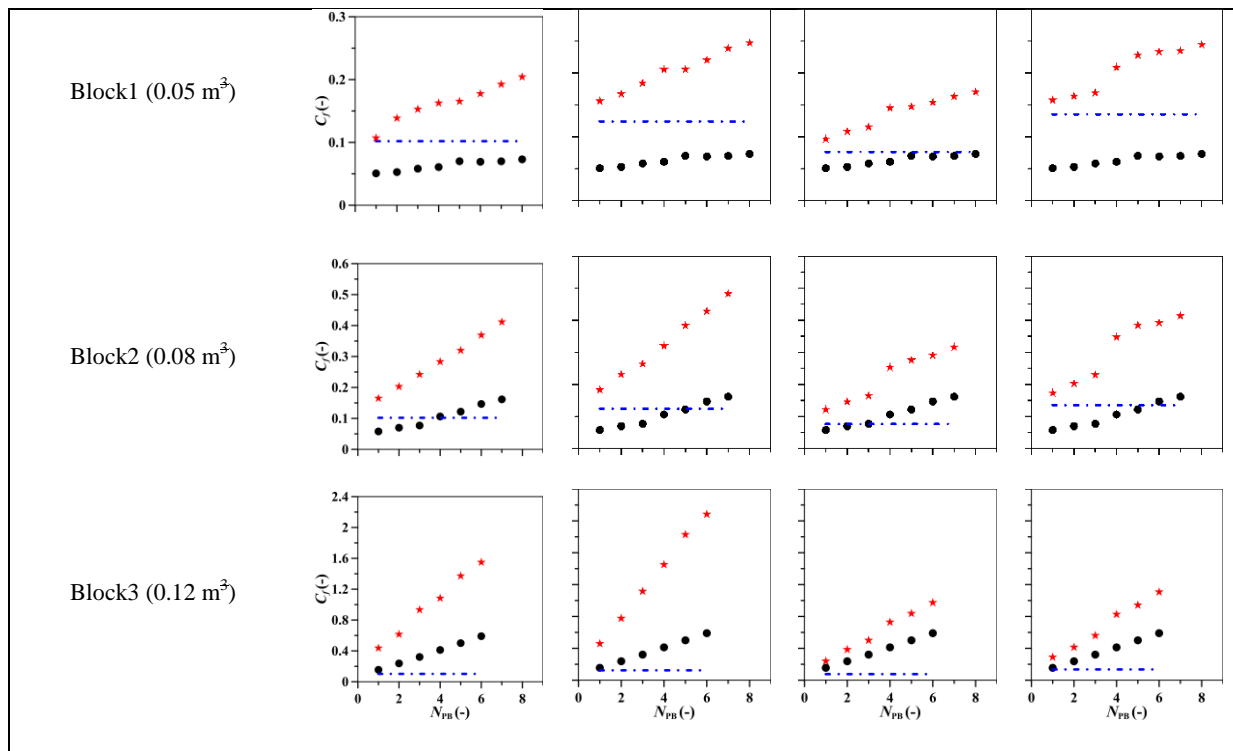


Fig. 12. Dimensionless pressure coefficient, C_f , evaluated in the presence of the blocks in the tunnel for both cases with and without barriers against the number of pairs of blocks, N_{PB} .

395 4.2.1 Tunnel with blocks but no barriers (i.e. circles in black)

396 It can be observed that: i) the pressure losses increase with the size of the blocks. As shown in the graphs, the pressure losses
 397 induced by all the small blocks placed in the tunnel (i.e. Block1) remain lower than those created by the barriers. Whereas
 398 those generated by one pair of large blocks (i.e. Block3) are already greater than to those created by the barriers. ii) The
 399 pressure losses increase with the number of cubes placed in the tunnel, in particular in the tunnel with large blocks where the
 400 growth is very pronounced. Based on these findings, it can be deduced that two parameters are connected with pressure
 401 losses: the blocking rate (i.e. ratio between blocking area and tunnel cross section) and the number of vehicles. Indeed, the
 402 higher the blocking rate and/or the number of vehicles, the greater the pressure losses.

403 4.2.2 Tunnel with blocks and barriers (i.e. stars in red)

404 **Fig. 12** clearly shows that the addition of barriers in a tunnel with vehicular blockages results in a significant increase in
 405 pressure loss. However, for small blocks (Block1), the highest values of dimensionless pressure coefficients are recorded in
 406 the two tunnel configurations "tunnel with small barriers $S = H$ " and "the tunnel with the largest barrier, $H/3$ ". Meanwhile,
 407 these dimensionless pressure coefficients are relatively small in the case of a tunnel with a large barrier, $H/4$. On the other
 408 hand, in the tunnel with large blocks (Block2 & Block3), the pressure losses induced by small barriers are much higher than
 409 those induced by each of the large barriers, especially in the case with the largest blocks (i.e. Block3). This is because the
 410 installation of several small barriers at the tunnel ceiling causes many changes and reductions within the tunnel cross sections
 411 and even more so in the case of a traffic jam, which consequently produces more singular pressure losses.

412 Comparing the two configurations of small barriers, we see that in the case where $S = 2H$, the pressure loss is less and
 413 therefore preferable for minimising the energy consumption of the ventilation system, on the one hand, and on the other more
 414 effective in reducing the critical velocity, according to the previous results reached in the first part of this study. Furthermore,
 415 **Fig. 9** and **Fig. 12** show that large barriers are more efficient and more reliable than small ones because they prevent the
 416 smoke backflow at greatly reduced critical velocities and they generate less loss pressure in the tunnels even in the situations
 417 with vehicular blockages.

5. CONCLUSIONS

418 Small-scale experiments were conducted in a reduced-scale tunnel to investigate the effects of solid barriers and blocks on
419 the behaviour of smoke in fire events within longitudinally ventilated tunnels. Two types of barriers fixed to the tunnel
420 ceiling were examined, small barriers with a height equal to $H/10$ and large barriers with heights equal to $H/4$ and $H/3$. The
421 vehicles in the tunnel are modelled by blocks of different sizes placed upstream of the buoyancy source. The smoke backflow
422 lengths, the critical velocities and the pressure losses were evaluated. The main conclusions are:

- 423 - The barriers prevent the back-layer flow from moving upstream of the source at low ventilation velocities (or at
424 least they reduce its length).
- 425 - The effectiveness of the barrier in preventing the smoke back-layering depends on its height, the greater the height
426 of the barrier, the more effective it is.
- 427 - The critical velocity is highly affected by the blocks located close to the source, while the effect of other blocks
428 placed further upstream of the source becomes negligible as the distance between the blocks and the source
429 increases.
- 430 - The reduction ratio of the critical velocity is very close to the reduction in cross-section of the tunnel induced by
431 the obstacles located close to the source (blocks, barriers or both), i.e. $1 - Rc = \varphi$.
- 432 - The effect of the barriers on the pressure loss is negligible compared to that induced by HGVs.
- 433 - The simultaneous presence of blocks and barriers in the tunnel leads to a large increase in pressure losses. This
434 increase is much greater with small barriers than with large barriers, especially when they are coupled with large
435 blocks.
- 436 - The large mobile barriers are much better than the small fixed barriers because they prevent the formation of the
437 back-layer flow at a much smaller ventilation velocity without generating excessive pressure losses.

438 In conclusion, ceiling barriers could help in improving safety in longitudinally ventilated road tunnels. This solution may be
439 particularly helpful, for example, in existing tunnels where the available space does not allow many jet fans to be installed, or
440 in tunnels with low traffic to reduce the renovation cost, as well as in some tunnels that require a strong thrust to achieve the
441 critical velocity, especially downhill tunnels where the adverse "chimney effect" is strong in case of fire. Therefore, by
442 reducing the critical velocity, barriers could help satisfy the ventilation objectives. However, positioning barriers inside the
443 tunnel might be challenging and the installation of mobile barriers requires an entire automated control system, as they are
444 designed to be deployed only in case of a fire, once detected. Finally, it is worth noting that the barrier heights investigated in
445 this paper are not necessarily optimal, and can be adjusted on a case-to-case basis.

446 Further studies could focus on the study of the behavior and control of smoke in the transverse ventilation tunnel, as well as
447 the impact of solid barriers on the performance of the extraction system.

448 ACKNOWLEDGMENTS

449 This work was supported by the Région Auvergne Rhône-Alpes and in partnership with Centre d'Etude des Tunnels (CETU).

450 **REFERENCES**

- 451 1 Y. Wu, M. Bakar, Control of smoke flow in tunnel fires using longitudinal ventilation systems - a study of the critical
452 velocity, *Fire Safety Journal*, vol. 35, pp. 363–390, 2000.
- 453 2 Heselden AJM. Studies of fire and smoke behaviour relevant to tunnels. Proceedings of the Second International
454 Symposium of Aerodynamics and Ventilation of Vehicle Tunnels, Paper J1, 1976.
- 455 3 Y. Oka, G.T. Atkinson, Control of smoke flow in tunnel fires, *Fire Saf. J.* 25 (1995) 305–322.
- 456 4 G.T. Atkinson, Y. Wu, Smoke control in sloping tunnels, *Fire Saf. J.* 27 (1996), pp. 335–341.
- 457 5 O. Mégret, O. Vauquelin, P. Chassé and E. Casalé, A reduced scale tunnel for the study of fire-induced smoke control,
458 3rd International Conference on Safety in Road and Rail Tunnels, ITC, Nice (1998).
- 459 6 L.H. Hu, R. Huo, H.B. Wang, Y.Z. Li, R.X. Yang, Experimental studies on fire-induced buoyant smoke temperature
460 distribution along tunnel ceiling, *Building and Environment* 42 (11) (2007) 3905–3915.
- 461 7 S. R. Lee, H. S. Ryou, A numerical study on smoke movement in longitudinal ventilation tunnel fires for different
462 aspect ratio, *Building and Environment*, 41(6) (2006) 719–725.
- 463 8 L.H. Hu, R. Huo, W.K. Chow, Studies on buoyancy-driven back-layering in tunnel fires, *Exp. Therm. Fluid Sci.* 32
464 (2008) 1468–1483.
- 465 9 Y.Z. Li, B. Lei, H. Ingason, Study of critical velocity and backlayering length in longitudinally ventilated tunnel fires,
466 *Fire Safety J.* 45 (2010) 361–370.
- 467 10 J.P. Kunsch, Critical velocity and range of a fire-gas plume in a ventilated tunnel, *Atmospheric Environment* 33 (1999)
468 13–24.
- 469 11 S.R. Lee, H.S. Ryou, An experimental study of the effect of the aspect ratio on the critical velocity in longitudinal
470 ventilation tunnel fires, *Journal of Fire Sciences* 23 (2005) 119–138.
- 471 12 O. Vauquelin, Parametrical study of the back flow occurrence in case of a buoyant release into a rectangular channel,
472 *Experimental Thermal and Fluid Science* 29 (2005) 725–731.
- 473 13 C.C. Hwang, J.C. Edwards, The critical ventilation velocity in tunnel fires--a computer simulation, *Fire Safety J.* 2005;
474 40(3): 213–244.
- 475 14 Kuang-Chung Tsai, Hon-Hsiang Chen, Shin-Ku Lee, Critical ventilation velocity for multi-source tunnel fires, *J. Wind
476 Eng. Ind. Aerodyn.* 98 (2010) 650–660.
- 477 15 J. S. Roh, S. S. Yang, H. S. Ryou, M. O. Yoon, Y. T. Jeong, An experimental study on the effect of ventilation velocity
478 on burning rate in tunnel fires—heptane pool fire case, *Building and Environment*, 43(7) (2008) 1225–1231.
- 479 16 G.B. Grant, S.F. Jagger, C.J. Lea, Fires in tunnels, *Philosophical Transactions of the Royal Society Theme Issue on Fire
480 Dynamics* 356 (1998) 2873–2906.
- 481 17 G.B. Grant, D. Drysdale, Estimating heat release rates from large-scale tunnel fires, in: *Fire Safety Science –
482 Proceedings of the Fifth International Symposium*, pp. 1213–1224.
- 483 18 Janssens, M., "Measuring Rate of Heat Release by Oxygen Consumption", *Fire Technology*, pp.234-249, August 1991.
- 484 19 Huggett, C., 1980. Estimation of the rate of heat release by means of oxygen consumption. *J. Fire Flammability* 12, 61–
485 65.
- 486 20 French, S.E., "EUREKA 499 - HGV Fire Test (Nov. 1992): Summary Report", Proceedings of the International
487 Conference on Fires in Tunnels, Borås, Sweden, October 10-11, Swedish National Testing and Research Institute: Fire
488 Technology, SP Report 1994:54.
- 489 21 Ingason, H., Lönnemark, A., 2005. Heat release rates from heavy goods vehicle trailer fires in tunnels. *Fire Safety
490 Journal* 40, 646–668.
- 491 22 P.H. Thomas, The movement of buoyant fluid against a stream and venting of underground fire, fire research station,
492 Watford, London, 1958.
- 493 23 J. Le Clanche, P. Salizzoni, M. Creyssels, R. Mehaddi, F. Candelier, O. Vauquelin, Aerodynamics of buoyant releases
494 within a longitudinally ventilated tunnel, *Experimental Thermal and Fluid Science* 57 (2014) 121–127.
- 495 24 G.R. Hunt, N.B. Kaye, Lazy plumes, *J. Fluid Mech.* 533 (2005) 329–338
- 496 25 B.R. Morton, Forced plumes, *J. Fluid Mech.* 5 (1959) 151–163.
- 497 26 P. H. Thomas, The movement of smoke in horizontal passages against an air flow, *Fire Research Note*, No. 723, Fire
498 Research Station, Watford, UK, 1968.
- 499 27 L. Jiang, M. Creyssels, A. Mos, P. Salizzoni, Critical velocity in ventilated tunnels in the case of fire plumes and
500 densimetric plumes, *Fire Safety Journal*, vol. 101, pp. 53–62, 2018.
- 501 28 P. Salizzoni, M. Creyssels, L. Jiang, A. Mos, R. Mehaddi, O. Vauquelin, Influence of source conditions and heat losses
502 on the upwind back-layering flow in a longitudinally ventilated tunnel, *International Journal of Heat and Mass Transfer*
503 117, 143–153, 2018.
- 504 29 D. Öttl, P. Sturm, R. Almbauer, W. Öttl, A. Turner, G. Seitlinger (2002), A new system to reduce the velocity of the air
505 flow in the case of fire, Proceedings of the Int. Conf. On Tunnel Safety and Ventilation, Graz, 8.-10.4.2002, 279–286.
- 506 30 M. Bettelini, S. Rigert, N. Seifert (2012), Flexible Devices for Smoke Control in Road Tunnels, 6th International
507 Conference 'Tunnel Safety and Ventilation' 2012, pp.265–272, Austria.
- 508 31 S. Rigert, M. Bettelini, New findings on the use of flexible curtains for smoke management in road tunnels, 15th
509 International Symposium on Aerodynamics, Ventilation & Fire in Tunnels 2013, pp.147–159, Barcelona, Spain.
- 510 32 M. Seike, N. Kawabata, & M. Hasegawa, The Effect of Fixed Smoke Barriers on Evacuation Environment in Road
511 Tunnel Fires with Natural Ventilation, 7th International Conference 'Tunnel Safety and Ventilation' 2014, Graz.
- 512 33 Y.P. Lee and K. C. Tsai, Effect of vehicular blockage on critical ventilation velocity and tunnel fire behavior in
513 longitudinally ventilated tunnels. *Fire Saf. J.*, 53:35–42, 2012.
- 514 34 W. Tang, L. H. Hu and L. F. Chen, Effect of blockage-fire distance on buoyancy driven back-layering length and critical
515 velocity in a tunnel: An experimental investigation and global correlations. *Appl. Therm. Eng.*, 60(1–2):7–14, 2013.

- 516 35 W. U. Rojas Alva, G. Jomaas and A. S. Dederichs, The influence of vehicular obstacles on longitudinal ventilation
517 control in tunnel fires. *Fire Saf. J.*, 87:25–36, 2017.
- 518 36 L. Jiang, Dynamics of densimetric plumes and fire plumes in ventilated tunnels, Ph.D. dissertation, Ecole Centrale de
519 Lyon, 2017.
- 520 37 S. Gannouni, R. B. Maad, Numerical study of the effect of blockage on critical velocity and backlayering length in
521 longitudinally ventilated tunnel fires, *Tunnelling and Underground Space Technology* 48, 147–155, 2015.
- 522 38 S. Zhang, X. Cheng, Y. Yao, K. Zhu, K. Li, S. Lu, R. Zhang, H. Zhang, An experimental investigation on blockage
523 effect of metro train on the smoke back-layering in subway tunnel fires, *Applied Thermal Engineering* 99, 214-223,
524 2016.
- 525 39 L. Jaing, M. Creyssels, G. R. Hunt and P. Silizzoni, Control of light gas releases in ventilated tunnels, *J. Fluid Mech.*,
526 accepted 2019, doi:10.1017/jfm.2019.363.
- 527 40 <http://www.bissistem.com/furness/files/FCO510-Laboratuvar-Tipi-Akis-Olcer.pdf>